PAPER

Check for updates

An examination of the relationship between molecular dipole moment and blood-gas partition for common anaesthetic gases†

Francisco A. Martins and Matheus P. Freitas 🆔 *

The solubility of inhalational anaesthetics in the bloodstream is related to the minimum alveolar concentration (MAC), which is an indicator of anaesthetic gas potency. The blood-gas partition coefficient (K_{bg}) is a measure of how much anaesthetics bind to plasma proteins in the blood compared to air. Just like the octanol–water partition coefficient, the K_{bg} may be related to the molecular dipole moment (μ), which can be modulated by the molecular conformation. Our quantum-chemical calculations demonstrated that subtle stereoelectronic interactions, namely those responsible for the anomeric and *gauche* effects, control the conformational equilibrium of some widely used volatile fluorinated anaesthetics and, consequently, of their molecular dipole moments. Since a remarkable correlation between empirical K_{bg} and calculated μ was found for these anaesthetics, the average molecular dipole moments may be used to predict the anaesthetic gas potency and other properties, such as lipid solubility, of inhalational anaesthetic analogs.

Introduction

The anaesthetic potency of inhalational anaesthetics appears to be dictated by the affinity of these compounds to plasma proteins in the blood, although their mechanism of action is not completely known and it may be a physical rather than a chemical bonding process.[1] To access these plasma proteins, the volatile anaesthetics should be reasonably soluble in the bloodstream and, therefore, the Ostwald coefficient for blood-gas, or simply the blood-gas partition coefficient (K_{bg}), can be a valuable descriptor for the prediction of the anaesthetic potency. The anaesthetic gas potency may be described by the minimum alveolar concentration (MAC), which is correlated to K_{bg} according to Fig. 1 for six last-generation fluorinated inhalational drugs.[2,3] However, the experimental measurement of K_{bg} may not be an easy task and, therefore, a straightforward method to obtain a parameter related to K_{bg} would be valuable for drug-likeness prediction purposes.

Linclau *et al.*[4] and then O'Hagan & Young[5] have recently found an interesting relationship between stereoelectronic effects and the lipophilicity of various fluorine-containing molecules, described as the octanol–water partition coefficient (log *P*). These studies demonstrated that the lipophilicity of a

molecule is related to its polarity, which is in turn governed by the molecular dipole moment (μ) balanced by the molecule's conformational populations. Since the conformational preferences of polar fluorocarbons are consistently driven by stereoelectronic effects, such as the fluorine *gauche* effect,[6] the authors concluded that lipophilicity informs on subtle stereo-
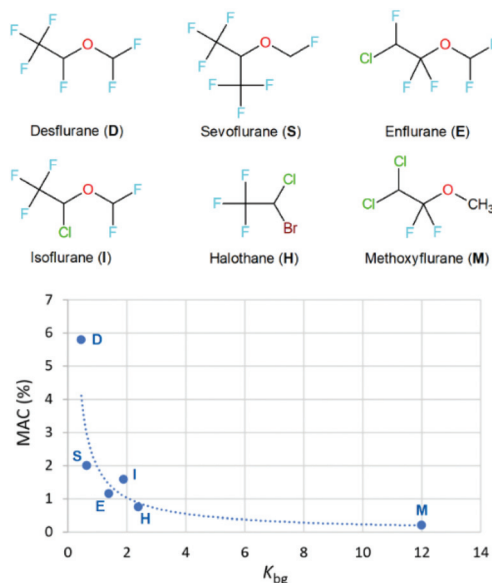

Fig. 1 Correlation between MAC (%) and blood-gas partition coefficients (K_{bg}) for six fluorinated inhalational anaesthetics (MAC = 1.958 × $K_{bg}^{-0.931}$, R^2 = 0.923).

Department of Chemistry, Institute of Natural Sciences, Federal University of Lavras, 37200-900 Lavras, MG, Brazil. E-mail: matheus@ufla.br

† Electronic supplementary information (ESI) available: Standard coordinates for the optimized geometries, dipole moments, K_{bg} data, and NBO energies. See DOI: 10.1039/d1ob01067k

This journal is © The Royal Society of Chemistry 2021

Org. Biomol. Chem., 2021, **19**, 6665–6670 | **6665**

electronic effects in fluorine chemistry. Indeed, the calculated average molecular dipole moments of a series of organofluorine herbicides have been properly correlated with the corresponding experimental $\log P$; such correlation was even better than that obtained from calculated $\log P$ values instead of μ.[7] Therefore, a similar approach may be used to analyze the relationship between polarity and the K_{bg} of key fluorinated inhalational anaesthetics.

The conformational behavior and experimental K_{bg} values for the six last-generation volatile anaesthetics of Fig. 1 are well-known.[2,3,8–12] Since most of them possesses oxygen electron lone pairs (n_O), electron-donating bonds (for example, C–H and C–C), and low-lying energy antibonding orbitals (for C–X, X = O, F, and Cl), some stereoelectronic interactions may appear to stabilize the conformations with geometric requirements for orbital overlapping, such as the *gauche* effect (*e.g.* due to $\sigma_{C-H/C-C} \rightarrow \sigma^*_{C-F}$ hyperconjugation) and the anomeric effect (*e.g.* due to $n_O \rightarrow \sigma^*_{C-F/C-Cl}$ electron delocalization).[13] Organofluorine compounds are remarkable in stereochemistry for exhibiting the fluorine *gauche* effect, whose benchmark is the 1,2-difluoroethane moiety. The surprising stability of its *gauche* conformer over the *anti* conformer is due especially to the antiperiplanar interactions between good electron-donating orbitals (σ_{C-H}) and low-lying energy electron-accepting
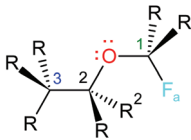
orbitals (σ^*_{C-F}).[14] In turn, the generalized anomeric effect that takes place in the O–C–X fragment-containing molecules (X = electronegative atom or group) is also importantly stabilizing if a $n_O \rightarrow \sigma^*_{C-X}$ electron delocalization is allowed.[15] These non-Lewis-type interactions counterbalance the Lewis-type contributions stemming from steric and electrostatic interactions, thus yielding the conformational energy differences.[16]

Therefore, the average molecular dipole moments for each fluorinated inhalational anaesthetic of Fig. 1 were obtained using *ab initio* calculations, rationalized in terms of the stereoelectronic interactions governing the conformational equilibria, and then correlated with K_{bg}. The outcomes may be useful for the modeling and prediction of new organofluorine compounds with anaesthetic properties.

Results and discussion

Whereas halothane (**H**) does not exhibit conformational isomerism, the remaining five fluorinated anaesthetics of Fig. 1 (**D**, **S**, **E**, **I**, and **M**) undergo rotation around the dihedral angles ϕ_1 (H–C$_1$–O–C$_2$), ϕ_2 (C$_1$–O–C$_2$–C$_3$), and ϕ_3 (O–C$_2$–C$_3$–H, for **E** and **M**). The conformational Gibbs free energies for the main conformers of each compound are given in Table 1, and

Table 1 Conformational Gibbs free energies (in kcal mol^{-1}) and population (%, in parenthesis), molecular dipole moments (μ, in Db), bond lengths (in Å), and dihedral angles (degrees) obtained for the main conformers of the studied fluorinated anaesthetic compounds (**C**)^a

C$\phi_1\phi_2\phi_3$	G^0_{rel} (%)	μ	O–C$_1$	C$_2$–O	C$_1$–F$_a$	C$_2$–R^2	Φ_1	Φ_2	Φ_3
H	— (100)	1.49	—	—	—	—	—	—	58.29
Esag	0.0 (21)	1.26	1.39	1.36	1.34	1.36	17.26	176.77	56.14
Es'a'g	0.1 (19)	0.45	1.39	1.37	1.34	1.35	340.46	185.33	57.62
Esag'	0.2 (14)	1.06	1.39	1.37	1.34	1.35	20.12	176.57	300.55
Es'a'g'	0.2 (14)	1.81	1.39	1.37	1.34	1.35	342.37	184.84	301.67
Es'a'a'	0.3 (13)	2.37	1.39	1.36	1.34	1.36	340.40	182.66	180.03
Esaa	0.3 (13)	2.51	1.39	1.36	1.34	1.36	19.33	174.25	178.90
Es'g'g'	1.6 (2)	1.48	1.39	1.38	1.34	1.35	353.25	282.10	302.91
Eg'gg	1.6 (1)	1.78	1.39	1.38	1.35	1.35	327.29	107.34	55.14
Esga	1.8 (1)	2.52	1.39	1.37	1.34	1.36	17.39	69.43	175.99
Eg'g'g	2.0 (1)	2.06	1.38	1.38	1.36	1.36	306.15	276.46	62.44
Egg'a	2.0 (1)	2.97	1.39	1.37	1.35	1.35	31.72	255.70	180.00
Iag	0.0 (61)	1.72	1.37	1.40	1.35	1.77	177.22	136.85	58.40
Iga	0.4 (31)	2.11	1.38	1.39	1.36	1.78	60.05	169.45	59.41
Ig'a	1.3 (7)	2.91	1.38	1.39	1.35	1.77	322.35	154.39	59.46
Is'g'	2.5 (1)	1.84	1.39	1.39	1.35	1.78	335.79	295.71	68.55
Dag	0.0 (76)	1.89	1.37	1.39	1.35	1.36	174.93	143.71	56.48
Dga	0.9 (18)	2.02	1.38	1.38	1.36	1.37	57.98	170.26	57.35
Dg'a	1.5 (5)	3.13	1.38	1.38	1.35	1.36	318.43	157.60	57.24
Ds'g'	2.9 (1)	1.59	1.39	1.38	1.35	1.37	336.92	296.68	67.23
Sgg	0.0 (100)	2.56	1.39	1.41	1.38	1.53	51.09	133.73	54.89
Mgaa	0.0 (58)	1.62	1.44	1.34	—	1.37	61.22	180.00	180.00
Mgag	0.2 (42)	2.62	1.44	1.35	—	1.36	59.25	179.07	57.60

^{a} Conformers for compounds **C** are named according to the dihedral angles ϕ_1, ϕ_2, and ϕ_3, which can be either *anti* (a and a', from 150° to 210°), *syn* (s and s', from 330° to 30°), or *gauche* (g and g', from 330° to 30°). The C$_1$–F$_a$ stands for the bond length involving the fluorine at anomeric orientation. The C–F, C–Cl, and C–Br bond lengths for halothane are 1.34, 1.76, and 1.91 Å, respectively.

6666 | *Org. Biomol. Chem.*, 2021, **19**, 6665–6670

This journal is © The Royal Society of Chemistry 2021

the optimized geometries for the whole series of compounds and respective conformers are shown in the ESI.† The overall molecular dipole moment of a molecule is the summation of the individual dipole moment vectors originated from the polar bonds. If this molecule experiences conformational isomerism, the resulting molecular dipole moment corresponds to an average value of the conformations. Considering that stereoelectronic effects rule the conformational preferences of compounds in the gas phase, thus the observed molecular dipole moments are also influenced by the stereoelectronic interactions operating in the system. It is worth mentioning that solvent effects on the conformational preferences are in general small for at least most of the studied compounds,[8–10] and, considering that implicit solvation calculations do not account properly for specific solute-solvent interactions (*e.g.* hydrogen bonding), only the molecular dipole moments obtained for the gas phase conformers will be considered.

Whereas compounds **E** and **M** have the requirements to experience the fluorine *gauche* effect, the compounds **D**, **S**, **I**, **E**, and **M** may present the anomeric effect. To gain insight into how these non-Lewis-type interactions contribute to the conformational electronic energies (E_{full}) of the studied compounds, the wavefunctions were localized with all natural bond orbitals (NBO) doubly occupied, and the resulting energy (E_L) was subtracted from E_{full} to give the electron delocalization energy E_{NL}, according to eqn (1) (Table 2).

$$E_{NL} = E_{full} - E_L \qquad (1)$$

E and **M** are capable of turning on the fluorine *gauche* effect through the $\sigma_{C-H} \to \sigma^*_{C-F}$ hyperconjugation along the ϕ_3 dihedral angle. However, since σ_{C-Cl} is a good electron-donating orbital but worse than σ_{C-H}, and σ^*_{C-O} is a good electron-accepting orbital but worse than σ^*_{C-F}, some competing interactions contribute to the rotation around the O–C_2–C_3–H dihedral angle in **E** and **M**. Considering that electron delocalizations from σ_{C-H} and to σ^*_{C-F} are only slightly more favoring than that from σ_{C-Cl} and to σ^*_{C-O} (see ESI†), the small differences in the rotational preferences for ϕ_3 are well explained by these stereoelectronic interactions. On the other hand, the anomeric effect appears in most of the studied systems (Table 2). The $n_O \to \sigma^*_{C-X}$ anomeric interactions are expected to shorten the C–O distance and lengthen the C–X bond. For instance, more stabilizing $n_O \to \sigma^*_{C-F}$ interactions in some conformers of **E** cause an increase in the respective C–F bonds of *ca.* 0.01 to 0.02 Å in a comparison with the conformers that experience weaker interactions. The effect of these interactions on the dihedral angles is also remarkable, once the bonds rotate to maximize the overlap between the orbitals involved in the anomeric interactions. Therefore, the stereoelectronic effects operating in these systems strongly affect the molecular geometries, conformer stabilities, and, consequently, the overall molecular dipole moment.

Compound **M** experiences both *gauche* and anomeric effects, but the overall contribution from the latter is weaker

Table 2 Lewis (L) and non-Lewis (NL) contributions to the full conformational electronic energies, and anomeric interactions for the rotationally flexible fluorinated anaesthetic compounds (**C**) studied herein (kcal mol^{-1})^a

C$\phi_1\phi_2\phi_3$	E_{full}	E_{NL}	E_L	$n_O \to \sigma^*_{C_1-F_a}$	$n_O \to \sigma^*_{C_2-CF3}$	$n_O \to \sigma^*_{C_2-F_a}$	$n_O \to \sigma^*_{C_2-Cl}$
Es*ag*	0.03	−2.27	2.30	13.31	—	32.44	—
Es′*a′g*	0.00	−1.96	1.96	13.67	—	32.38	—
Es*ag′*	0.17	−2.05	2.22	13.73	—	31.78	—
Es′*a′g′*	0.22	−2.48	2.70	13.52	—	31.83	—
Es′*a′a′*	0.18	−3.58	3.76	13.62	—	33.56	—
Es*aa*	0.19	−3.79	3.98	13.73	—	33.52	—
Es′*g′g′*	1.18	−0.86	2.04	11.83	—	20.36	—
Eg′*gg*	1.33	−2.05	3.38	15.92	—	20.12	—
Es*ga*	1.24	−2.78	4.02	13.86	—	22.03	—
Eg′*g′g*	1.65	0.00	1.65	15.48	—	18.92	—
Eg*g′a*	1.67	−3.44	5.11	15.94	—	20.71	—
Ia*g*	0.00	0.00	0.00	13.07	—	—	13.09
Ig*a*	0.21	−0.75	0.96	12.55	—	—	16.28
Ig′*a*	1.93	−6.10	8.03	16.17	—	—	16.15
Is′*g′*	1.92	−6.04	7.96	15.38	—	—	15.66
Da*g*	0.00	−1.79	1.79	13.70	—	16.20	—
Dg*a*	0.90	0.00	0.90	13.48	—	17.21	—
Dg′*a*	1.90	−8.97	10.87	16.57	—	18.41	—
Ds′*g′*	2.34	−6.75	9.09	15.34	—	15.67	—
Sg*g*	0.00	0.00	0.00	15.78	8.84	—	—
Mg*aa*	0.00	−1.91	1.91	—	—	39.18	—
Mg*ag*	0.29	0.00	0.29	—	—	37.15	—

^{a} The $n_O \to \sigma^*_{C_1-F_a}$ interaction corresponds to the contribution involving the fluorine at anomeric orientation; $n_O \to \sigma^*_{C_2-CF3}$ corresponds only to the antiperiplanar interaction; $n_O \to \sigma^*_{C_2-CF}$ corresponds to the sum of these interaction energies for the two C–F bonds when possible (for **E** and **M**).

This journal is © The Royal Society of Chemistry 2021

Org. Biomol. Chem., 2021, **19**, 6665–6670 | **6667**

than in **E** because C-1 is not attached to any fluorine. On the other hand, the two fluorine atoms at C-2 allow for an effective *gauche* effect. These two factors lead **M** to a preferential conformational behaviour in which all bonds are staggered. For the remaining molecules **D**, **S**, and **I**, there is a competition between the $n_O \rightarrow \sigma^*_{C_1-R_1}$ (leading to a *syn* ϕ_1) and $n_O \rightarrow \sigma^*_{C_2-R_2}$ interactions (leading to a *gauche* ϕ_2). Compound **S** bears a worse R^2-containing electron-accepting orbital (σ^*_{C-CF3}) compared to **D** and **I**, leading to less stabilizing $n_O \rightarrow \sigma^*_{C_2-R_2}$ interactions in **S** than in **D** and **I**. Even though, compound **S** presents a single stable conformer in the gas phase, whereas the conformers with a *gauche* ϕ_2 dominate the conformational equilibrium in **D** (**D**ag) and **I** (**I**ag). According to the energy decomposition analysis of Table 2, this behaviour is due to a balance of Lewis and non-Lewis-type interactions; whereas the single stable conformer of **S** is substantially more favoured than its metastable conformers due to a large $E_{NL} - E_L$ energy difference, both **D**ag and **I**ag are little destabilized by steric effects but also only slightly stabilized by electron delocalization, leading to a non-monotonic conformational equilibrium. The six geometries corresponding to the most stable conformer in the gas phase for each compound, which are consistent with the literature,[8–12] are shown in Fig. 2.

Considering that the molecular polarity of organofluorine compounds is related to their octanol–water partition coefficient,[4,5,7,17] as well as that blood is mostly constituted by water,[18] the solubility of fluorinated anaesthetics in the bloodstream, described in terms of the blood-gas partition coefficient, may be correlated to the average molecular dipole moment. At first glance, compound **M** demonstrates an outlier behaviour due to its exceedingly high K_{bg} of 12 for an average μ of 2.04 Db (see discussion on vapour pressure further in this discussion). Nevertheless, it is worth mentioning that other factors than binding to plasma proteins may appear to set anaesthetic molecules in the blood, such as the affinity to red blood cells.[19] Accordingly, the average dipole moments for the remaining five fluorinated anaesthetics were plotted against the respective K_{bg} values (Fig. 3), yielding a determination coefficient R^2 of 0.65, which is acceptable for quantitative structure–activity relationship purposes.[20] Yet, considering
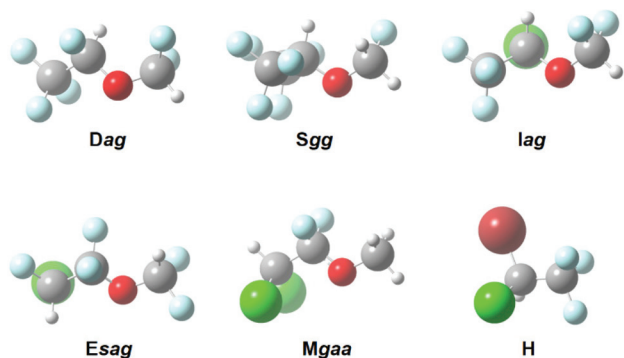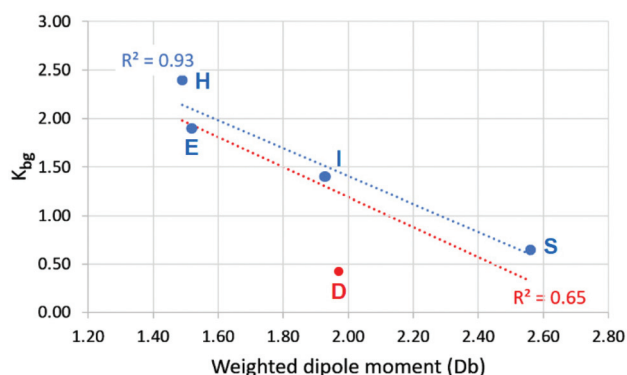
Fig. 3 Linear correlation plots of average dipole moments (μ) *versus* blood-gas partition coefficients (K_{bg}) for **H**, **E**, **S**, and **I** (blue line) and also including **D** (red line). $K_{bg} = -1.4417\mu + 4.2907$ (blue line); $K_{bg} = -1.5463\mu + 4.2811$ (red line).

that **D** appears to abnormally influence the regression line, the resulting plot obtained after exclusion of this compound gives an impressive correlation with $R^2 = 0.93$. Although the origin of this outlier behaviour is not clear, it is worth considering an effect of the vapour pressure, which is considerably higher for **D** (667.6 mmHg)[21] in a comparison with **S** (157.5 mmHg),[22] **I** (240.0 mmHg),[23] **E** (174.5 mmHg),[24] **M** (22.5 mmHg),[25] and **H** (243.0 mmHg)[26] at 20 °C.

Computational methods

The geometries corresponding to all possible staggered conformations depicted in Fig. 4 were fully optimized and the absence of imaginary frequencies was checked to guarantee that the located conformers were real energy minima. These procedures were performed at the *ab initio* MP2/aug-cc-pVTZ level of theory[27–30] using the Gaussian 09 program.[31] The calculations were carried out using the default integration grid of G09: FineGrid, with 75 radial shells and 302 angular points per shell. The geometries for the main conformers (*i.e.* those with Gibbs population of at least 1% in the gas phase) were consistent with the structures available in the literature[8–12] and, therefore, the molecular dipole moments considered to build a correlation with the experimental blood-gas partition coefficients[2,3] were weighted by these populations. The MP2-derived dipole moments have been demonstrated to be reliable and accurate.[32] The electron delocalization and Lewis-type contributions to the conformational energies were obtained through second-order perturbation analysis of donor–acceptor interactions in the natural bond orbitals (NBO).[16] The Lewis-type energy (E_L) results from the perfectly localized NBÓs and nearly represents the steric energy between doubly occupied orbitals, which is higher than the original energy (E_{full}). The non-Lewis type energy (E_{NL}) corresponds to the stabilizing effect of delocalizing contributions. The NBO calculations were performed using density functional theory at the B3LYP/
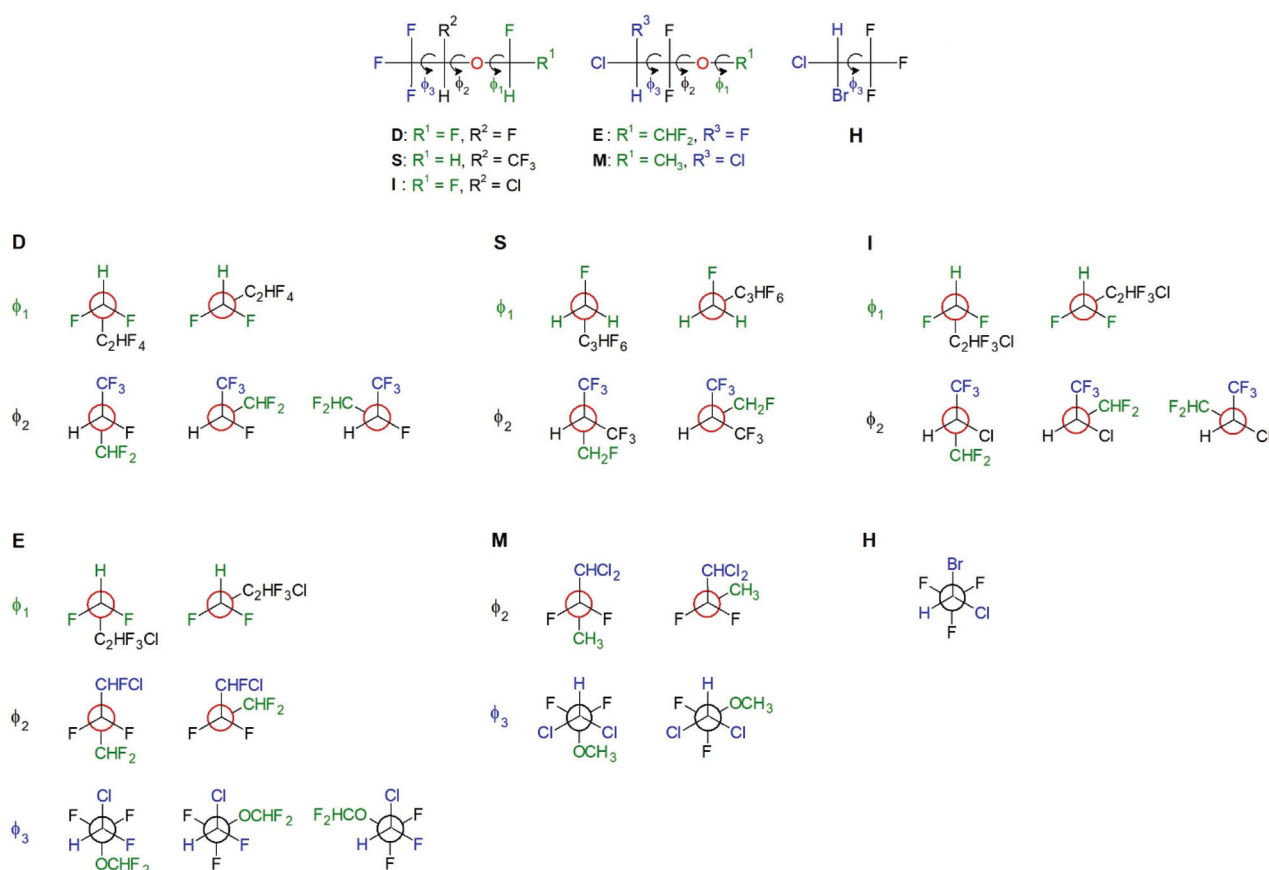
Fig. 2 Most stable conformer for each halogenated anaesthetic.

6668 | *Org. Biomol. Chem.*, 2021, **19**, 6665–6670

This journal is © The Royal Society of Chemistry 2021

Fig. 4 Staggered conformations for each dihedral angle of the six fluorinated anaesthetics studied herein.

aug-cc-pVTZ level of theory,[33,34] including the empirical dispersion corrections proposed by Grimme and co-workers.[35,36]

Conclusions

The conformational equilibrium of five fluorinated anaesthetics was discussed in terms of electron delocalization and Lewis-type interactions. Although the classical steric and electrostatic interactions contribute to the conformational balance, the stereoelectronic interactions that rule the anomeric and *gauche* effects appeared to stabilize some conformers with specific geometries more than others. Because each conformer has a given dipole moment, the overall molecular dipole moment μ is a combination of the individual dipole moments balanced by the respective conformer populations. We found a linear dependence of K_{bg} with these average dipole moments for **H**, **E**, **I**, **S**, and **D**, which greatly improves if **D** is removed from the regression. This demonstrates the importance of this parameter for rational drug design. Although the K_{bg} of **M** and **D** may be affected by other physical or chemical mechanisms than the solubility of the anaesthetic in the bloodstream and their interaction with the blood plasma proteins, our findings open the possibility to describe crucial pharmacokinetic data by an easily accessible quantum-chemical parameter.

Author contributions

F. A. Martins: investigation, original draft; M. P. Freitas: review & editing, supervision.

Conflicts of interest

There are no conflicts to declare.

Acknowledgements

This journal is © The Royal Society of Chemistry 2021

Org. Biomol. Chem., 2021, **19**, 6665–6670 | **6669**

Notes and references

1 J. Travis, *Sci. News*, 2004, **166**, 8.

2 J. J. Nagelhout and S. Elisha, *Nurse Anesthesia*, Elsevier, Amsterdam, 6th edn, 2017.

3 J. F. Butterworth, J. D. Wasnick and D. C. Mackey, *Morgan & Mikhail's Clinical Anesthesiology*, McGraw-Hill Education, New York, 6th edn, 2018.

4 B. Linclau, Z. Wang, G. Compain, V. Paumelle, C. Fontenelle, N. Wells and A. Weymouth-Wilson, *Angew. Chem., Int. Ed.*, 2016, **55**, 674.

5 D. O'Hagan and R. J. Young, *Angew. Chem., Int. Ed.*, 2016, **55**, 3858.

6 D. Y. Buissonneaud, T. van Mourik and D. O'Hagan, *Tetrahedron*, 2010, **66**, 2196.

7 D. R. Silva, J. K. Daré and M. P. Freitas, *Beilstein J. Org. Chem.*, 2020, **16**, 2469.

8 M. P. Freitas, M. Bühl, D. O'Hagan, R. A. Cormanich and C. F. Tormena, *J. Phys. Chem. A*, 2012, **116**, 1677.

9 L. A. F. Andrade, J. M. Silla, S. L. Stephens, K. Marat, E. F. F. da Cunha, T. C. Ramalho, J. van Wijngaarden and M. P. Freitas, *J. Phys. Chem. A*, 2015, **119**, 10735.

10 M. C. Guimarães, M. H. Duarte, J. M. Silla and M. P. Freitas, *Beilstein J. Org. Chem.*, 2016, **12**, 760.

11 S. M. Milikova, K. S. Rutkowski, B. Czarnik-Matusewicz and M. Rospenk, *Chem. Phys. Lett.*, 2015, **637**, 77.

12 Y. S. Li and J. R. Durig, *J. Mol. Struct.*, 1982, **81**, 181.

13 I. V. Alabugin, *Stereoelectronic Effects*, Wiley, Chichester, 2016.

14 D. R. Silva, L. A. Santos, T. A. Hamlin, C. F. Guerra, M. P. Freitas and F. M. Bickelhaupt, *ChemPhysChem*, 2021, **22**, 641.

15 M. P. Freitas, *Org. Biomol. Chem.*, 2013, **11**, 2885.

16 F. Weinhold and C. R. Landis, *Discovering Chemistry with Natural Bond Orbitals*, Wiley, Hoboken, 2012.

17 B. F. J. Jeffries, Z. Wang, H. R. Felstead, J.-Y. Le Questel, J. Scott, E. Chiarparin, J. Graton and B. Linclau, *J. Med. Chem.*, 2020, **63**, 1002.

18 H. P. Wright, *Br. Med. J.*, 1953, **2**, 1312.

19 K. S. Khan, I. Hayes and D. J. Buggy, *Contin. Educ. Anaesth. Crit. Care Pain*, 2013, **14**, 106.

20 R. Todeschini, V. Consonni, D. Ballabio and F. Grisoni, in *Comprehensive Chemometrics*, ed. S. D. Brown, R. Tauler and B. Walczak, Elsevier, Amsterdam, 2020, pp. 599–634.

21 M. J. O'Neil, *The Merck Index – An Encyclopedia of Chemicals, Drugs, and Biologicals*, Whitehouse Station, Merck and Co., Inc., 2006.

22 International Labour Organization, https://www.ilo.org/dyn/icsc/showcard.display?p_version=2&p_card_id=1436.

23 International Labour Organization, https://www.ilo.org/dyn/icsc/showcard.display?p_version=2&p_card_id=1435.

24 R. J. Lewis Sr, *Hawley's Condensed Chemical Dictionary*, John Wiley & Sons, Inc., New York, 2007.

25 International Labour Organization, https://www.ilo.org/dyn/icsc/showcard.display?p_version=2&p_card_id=1636.

26 International Labour Organization, https://www.ilo.org/dyn/icsc/showcard.display?p_version=2&p_card_id=0277.

27 M. J. Frisch, M. Head-Gordon and J. A. Pople, *Chem. Phys. Lett.*, 1990, **166**, 275.

28 M. Head-Gordon, J. A. Pople and M. J. Frisch, *Chem. Phys. Lett.*, 1988, **153**, 503.

29 R. A. Kendall, T. H. Dunning and R. J. Harrison, *J. Chem. Phys.*, 1992, **96**, 6796.

30 P. A. Fantin, P. L. Barbieri, A. C. Neto and F. E. Jorge, *J. Mol. Struct.: THEOCHEM*, 2007, **810**, 103.

31 M. J. Frisch, G. W. Trucks, H. B. Schlegel, G. E. Scuseria, M. A. Robb, J. R. Cheeseman, G. Scalmani, V. Barone, G. A. Petersson, H. Nakatsuji, X. Li, M. Caricato, A. Marenich, J. Bloino, B. G. Janesko, R. Gomperts, B. Mennucci, H. P. Hratchian, J. V. Ortiz, A. F. Izmaylov, J. L. Sonnenberg, D. Williams-Young, F. Ding, F. Lipparini, F. Egidi, J. Goings, B. Peng, A. Petrone, T. Henderson, D. Ranasinghe, V. G. Zakrzewski, J. Gao, N. Rega, G. Zheng, W. Liang, M. Hada, M. Ehara, K. Toyota, R. Fukuda, J. Hasegawa, M. Ishida, T. Nakajima, Y. Honda, O. Kitao, H. Nakai, T. Vreven, K. Throssell, J. A. Montgomery Jr., J. E. Peralta, F. Ogliaro, M. Bearpark, J. J. Heyd, E. Brothers, K. N. Kudin, V. N. Staroverov, T. Keith, R. Kobayashi, J. Normand, K. Raghavachari, A. Rendell, J. C. Burant, S. S. Iyengar, J. Tomasi, M. Cossi, J. M. Millam, M. Klene, C. Adamo, R. Cammi, J. W. Ochterski, R. L. Martin, K. Morokuma, O. Farkas, J. B. Foresman and D. J. Fox, *Gaussian 09, Revision D.01*, Gaussian, Inc., Wallingford, 2016.

32 E. D. Simandiras, R. D. Amos and N. C. Handy, *Chem. Phys.*, 1987, **114**, 9.

33 A. D. Becke, *J. Chem. Phys.*, 1993, **98**, 5648.

34 R. A. Kendall, T. H. Dunning and R. J. Harrison, *J. Chem. Phys.*, 1992, **96**, 6796.

35 S. Grimme, S. Ehrlich and L. Goerigk, *J. Comput. Chem.*, 2011, **32**, 1456.

36 E. R. Johnson and A. D. Becke, *J. Chem. Phys.*, 2005, **123**, 024101.

6670 | *Org. Biomol. Chem.*, 2021, **19**, 6665–6670

This journal is © The Royal Society of Chemistry 2021